A comprehensive assessment of gait accelerometry signals in time, frequency and time-frequency domains

Ervin Sejdić* Kristin A. Lowry† Jennica Bellanca‡ Mark S. Redfern
Jennifer S. Brach§

Abstract

Gait accelerometry is a promising tool to assess human walking and reveal deteriorating gait characteristics in patients and can be a rich source of clinically relevant information about functional declines in older adults. Therefore, in this paper, we propose a comprehensive set of signal features that may be used to extract clinically valuable information from gait accelerometry signals. To achieve our goal, we collected tri-axial gait accelerometry signals from 35 adults 65 years of age and older. Fourteen subjects were healthy controls, ten participants were diagnosed with Parkinson's disease and eleven participants were diagnosed with peripheral neuropathy. The data were collected while the participants walked on a treadmill at a preferred walking speed. Accelerometer signal features in time, frequency and time-frequency domains were extracted. The results of our analysis showed that some of the extracted features were able to differentiate between healthy and clinical populations. Signal features in all three domains were able to emphasize variability among different groups, and also revealed valuable information about variability of the signals between anterior-posterior, mediolateral and vertical directions within subjects. The current results imply that the proposed signal features can be valuable tools for the analysis of gait accelerometry data and should be utilized in future studies.

Keywords: Gait accelerometry, signal features, time domain, frequency domain, time-frequency domain, healthy older adults, peripheral neuropathy, Parkinson's disease.

*Ervin Sejdić is with the Department of Electrical and Computer Engineering, Swanson School of Engineering, University of Pittsburgh, Pittsburgh, PA, 15261, USA. E-mail: esejdic@ieee.org.

†Kristin A. Lowry is with the Department of Medicine, Division of Geriatrics, University of Pittsburgh, Pittsburgh, PA, 15261, USA. E-mail: kal121@pitt.edu.

‡Jennica Bellanca and Mark S. Redfern are with the Department of Biomedical Engineering, Swanson School of Engineering, University of Pittsburgh, Pittsburgh, PA, 15261, USA. E-mail: mredfern@pitt.edu.

§Jennifer S. Brach is with the Department of Physical Therapy, University of Pittsburgh, Pittsburgh, PA, 15260, USA. E-mail: jbrach@pitt.edu.

1 Introduction

Loss of independence is a major factor of mobility disability in older adults, which also increases morbidity and mortality in older adults [1]. Hence, walking and its related metrics (e.g. gait speed, cadence, step length, step width, variability) have been previously considered as they are predictive of self-rated health status [2], general cognitive function and dementia (e.g., [3], [4]), as well as morbidity and mortality [1]. Additionally, older adults with central dysfunction such as Parkinson's disease (PD) and peripheral dysfunction such as Peripheral Neuropathy (PN) show even higher rates of disordered walking, instability and falls [5], [6]. While important indicators of overall function, simple gait metrics have shown to be limited in their ability to discriminate between age- and disease related gait dysfunction, such as for older adults versus early stages of PD [7], [8], or between those who do and do not fall within PD and PN cohorts [9], [10]. Clinical trials to improve walking ability generally focus on normalizing gait metrics; however, in clinical groups such as PD, these improvements do not necessarily coincide with improved motor control [11]. Thus, there is need for outcome measures that will indicate changes in locomotor mechanisms not detected by simple gait metrics.

Various sensors have been used to assess gait over the years (e.g., [12], [13]). The quantification of gait patterns via accelerometers has become popular in recent years due to improved measurement accuracy, ease, and affordability of accelerometers. Gait acceleration data have demonstrated good measurement reliability across days [14], with changes in gait speed [15], changes in walking surface [16], and with different anatomical placement of the accelerometer, including placement at the trunk. As the trunk segment comprises over half of the mass of the body, researchers have suggested that control of the trunk is prioritized by the nervous system [17], [18]. In support, measures of trunk dynamics have shown to be more sensitive to age- and disease-related gait changes than lower extremity and spatiotemporal measures [19], [20], [21]. Measures derived from lower trunk accelerations, considered to be proxy center-of-mass accelerations, have been proposed as global indicators of the motor control of walking [22].

The sensitivity of acceleration measurement allows for extraction of multiple signal features that have been used in other biomedical applications (e.g., [23], [24]). Previous studies using accelerometry have generally compared the discriminatory ability of one acceleration feature against typical spatiotemporal footfall data (gait speed, cadence, step length/width) (e.g., [7]). Few studies have examined multiple acceleration features within the same sample (e.g., [25]), and to date, no study has comprehensively examined multiple gait accelerometry features across healthy and clinical groups.

The purpose of this study was to explore the feasibility and usefulness of extracting features from multiple signal domains from trunk accelerometry signals in both healthy and clinical groups. We studied neurologically intact older adults, and individuals with PD and PN because we anticipated contrasting abnormalities in gait performance, as these disorders differ in central and peripheral neurologic factors that influence gait performance [26]. Specifically, we explored features in time, frequency and time-frequency domains. The results of this study provide insights into how these additional signal features can be used to differentiate between the three considered groups and how the features can possibly be used to identify changes during

different walking conditions.

2 Methods

2.1 Data acquisition

Thirty five, adults age 65 years of age and older were recruited for this study which was approved by the Institutional Review Board at the University of Pittsburgh. The participants included 14 healthy controls (HC), 10 with Parkinson's disease (PD) and 11 with peripheral neuropathy (PN). All individuals were ambulatory without an assistive device or the assistance of another person and were able to continuously walk for at least 3 minutes. All subjects were assessed using a structured history and physical exam to ensure they meet the general inclusion/exclusion criteria for the study. Potential subjects were excluded if they had any undiagnosed neurological (e.g. abnormal neurological examination such as spasticity, or severe paresis), musculoskeletal, cardiopulmonary conditions or inadequate hearing or vision that would interfere with the tasks of the study. Additionally, eligibility for HCs required no diagnosed neurological, vestibular or sensory disorders and biothesiometer reading ≤ 20 at the bilateral malleolus. PDs were required to have had a diagnosis of Parkinson's disease for at least one year according to a Hoehn and Yahr scale rating of 2 or 3 and a bioesthesiometer reading ≤ 20 at the bilateral malleolus. All PD subjects were on a stable dosing schedule of Parkinson's medications for at least three months prior to testing. Subjects with PN were required to have a biothesiometer reading ≥ 40 at the bilateral malleolus, indicating a loss of vibratory sense. The data presented here were part of a larger project that examined postural control in both standing and walking in 3 groups with distinct balance abilities. Subjects meeting inclusion criteria completed clinical assessments of balance, strength, and overground walking, as well as three-dimensional motion analysis of standing balance and walking.

Walking trials were performed on a large custom computer-controlled treadmill (1.2 m wide by 2 m long) with a safety harness system. A 3-D optical motion capture system (Natural Point, Inc) was used to collect trajectory data during gait. Subjects were outfitted with 39 (31 dynamic and 8 static) reflective markers placed on the bony landmarks, as seen in Figure 1 (the large marker set was required to meet the objectives of the larger study). For the purpose of this investigation, only the heel and toe trajectory data were used for stride segmentation. Linear acceleration of the body was measured along vertical (V), anterior-posterior (AP) and medial-lateral (ML) axes using a tri-axial accelerometer (MMA7260Q, Freescale Semiconductor) firmly secured over the L3 segment of the lumbar spine as shown in Figure 2. The accelerometer was attached using a belt, and a 4 inch wide elastic bandage wrapped over the accelerometer and around the trunk to firmly attach it to the body. Trunk accelerations were sampled at 100 Hz. Each walking trial began with a ramp up period, where the subject's walking speed was slowly increased until the preferred speed determined earlier was reached. Once the preferred gait speed was achieved, subjects completed a 3-minute walking trial on the treadmill at their normal (preferred) walking speed.

2.2 Data pre-processing

Using the motion capture data from the toe (MTOE as shown in Figure 1) and heel (HEEL as shown in Figure 1), we segmented the trajectory data intro strides according to the algorithm in [27].

2.3 Feature extraction

From the stride segmented data, we extracted gait speed, mean stride intervals (MSI) and coefficients of variations (CV) (e.g., [28], [29]). Also, using the stride segmented trajectories, we extracted the largest Lyapunov exponents (λ_L) (e.g., [28]) and harmonic ratios (HR) (e.g., [22]) from the acceleration signals:

- The maximum Lyapunov exponent, λ_L, is used to assess local stability. λ_L denotes the sensitivity of the system to small perturbations and the dependence of the system on initial conditions. To calculate λ_L, we used the recorded signal values, $x(n)$, and formed the state-space representations:

$$Z(n) = [x(n), x(n+T), x(n+T), ..., x(n+(d_E-1)T)] \tag{1}$$

  where $Z(n)$ is the d_E-dimensional state vector, T is the time delay, and d_E is the embedding dimension. The autocorrelation function approach was utilized to estimate the the time delay [30]. The global false nearest neighbor analysis was employed for the estimation of the embedding dimension [31]. $d_E = 5$ was set to five as recommended in previous publications [28], [32]. For finite-length signals, the maximum finite-time Lyapunov exponents was estimated using the following relationship [32]:

$$\ln(d_j(i)) \approx \lambda_L + \ln(D_j) \tag{2}$$

  where $d_j(i)$ was the Euclidean distance between the j^{th} pair of nearest neighbors after i discrete time steps and D is the initial average separation between neighboring trajectories. The slopes of curves defined by:

$$y(i) = \frac{1}{\Delta t}\langle \ln(d_j(i)) \rangle \tag{3}$$

  were used to estimate λ_L. Here, $\langle \ln(d_j(i)) \rangle$ denotes the average over all values of j. Specifically, λ_L represents the slope of $y(i)$ between forth and tenth strides.

- The harmonic ratios were calculated in each anatomical direction from low pass filtered acceleration data over each stride. The cutoff frequency of the low pass filter was set to 30 Hz. First, we calculated the discrete Fourier transform of the segmented data as follows (e.g., [27], [33]):

$$a_{stride} = \sum_{n=0}^{N-1} C_n \sin(n\omega_o t + \phi_n) \tag{4}$$

  where the C_n is the harmonic coefficient, ω_o is the stride frequency, and ϕ_n is the phase. The first 20

harmonic coefficients are then summed and used to calculate the harmonic ratio, which is defined as:

$$HR_{\text{AP and V}} = \left\langle \frac{\sum_{n=2,4,6,\ldots}^{20} C_n}{\sum_{n=1,3,5,\ldots}^{19} C_n} \right\rangle \tag{5}$$

$$HR_{ML} = \left\langle \frac{\sum_{n=2,4,6,\ldots}^{20} C_n}{\sum_{n=1,3,5,\ldots}^{19} C_n} \right\rangle \tag{6}$$

where $\langle \sum C_n / \sum C_n \rangle$ denotes the average ratio over all strides. This metric allows us to quantify the step to step asymmetry in the acceleration at the L3/L4, which has been used as a proxy center of mass.

2.3.1 Statistical features

Using only acceleration signals we extracted a number of different features from each of the three directions. Considering a signal $X = \{x_1, x_2, \ldots, x_n\}$, the following statistical features (e.g., [34]) were extracted:

- An unbiased estimate of the standard deviation was computed as follows:

$$\sigma_X = \sqrt{\frac{1}{n-1}\sum_{i=1}^{n}(x_i - \mu_X)^2} \tag{7}$$

  where μ_X denotes the mean of the signal. Standard deviation of the signal amplitude measures the spread of the amplitude distribution and its squared values is related to the AC signal power. Greater values of the standard deviation represent that the data points are spread over a larger interval of values.

- The skewness was computed as follows:

$$\xi_X = \frac{\frac{1}{n}\sum_{i=1}^{n}(x_i - \mu_X)^3}{\left\{\frac{1}{n}\sum_{i=1}^{n}(x_i - \mu_X)^2\right\}^{3/2}} \tag{8}$$

  and it measures the asymmetry of the amplitude distribution . A zero value indicates that the data points are evenly distributed on both sides, while negative/positive values indicated that more points lie right/left from the mean.

- The kurtosis given by:

$$\gamma_X = \frac{\frac{1}{n}\sum_{i=1}^{n}(x_i - \mu_X)^4}{\left\{\frac{1}{n}\sum_{i=1}^{n}(x_i - \mu_X)^2\right\}^{2}} \tag{9}$$

  measures how the amplitude distribution decays slowly near the extremes. In other words, higher values of kurtosis indicate that that variance stems from infrequent extreme deviations.

- The zeroth-lag cross-correlation coefficient between two signals was computed as follows:

$$\eta_{XY} = \frac{\sum_{i=1}^{n}(x_i - \mu_X)(y_i - \mu_Y)}{\sqrt{\sum_{i=1}^{n}(x_i - \mu_X)^2}\sqrt{\sum_{i=1}^{n}(y_i - \mu_Y)^2}} \tag{10}$$

  where μ_X and μ_Y denote the mean of a signal. η_{XY} measures the similarity of two signals, where zero indicates no similarity between two signals, while one indicates that the signals are identical.

2.3.2 Information-theoretic features

Information-theoretic features, which are often used in the analysis of biomedical signals (e.g., [24], [35], [36]), were calculated.

- To assess the predictability of the signal, we utilized a measure from information theory known as the Lempel-Ziv complexity (LZC) [35], [37], [38]. As the first step, the signal was converted into 100 symbols via 99 thresholds. Next, the quantized signal was decomposed into k blocks, which were used to compute the normalized LZC as follows [38]:

$$LZC = \frac{k \log_{100} n}{n}. \tag{11}$$

  Given that the signal was quantized into 100 symbols, the logarithmic base of 100 was used in this manuscript. Larger values of LZC indicate more complex data.

- Regularity of a signal was assessed via the entropy rate (ρ) [36], [39], as it is anticipated that consecutive data points related. Values of X, initially normalized by subtracting μ_X and dividing by σ_X, were quantized into 10 equally spaced levels. Next, sequences of $10 \leq R \leq 30$ consecutive points in $\widehat{X}$ were coded as a series of integers, $\Upsilon_R = \{u_1, u_2, ..., u_{n-R+1}\}$, using the following rule:

$$u_i = 10^{R-1}\widehat{x}_{i+R-1} + 10^{R-2}\widehat{x}_{i+R-2} + ... + 10^0\widehat{x}_i \tag{12}$$

  As there were 10 quantization levels, u_i values ranged from 0 to $10^R - 1$. To calculate the Shannon entropy, Δ , of Υ_R, we used the following relation:

$$\Delta(R) = \sum_{q=0}^{10^R-1} p_{\Upsilon_R}(q) \ln p_{\Upsilon_R}(q) \tag{13}$$

  where $p_{\Upsilon_R}(j)$ represents the approximated probability of the value q in Υ_R. To quantify regularity, we first computed the normalized entropy rate, $\widetilde{\Delta}$ as follows:

$$\widetilde{\Delta}(R) = \frac{\Delta(R) - \Delta(R-1) + \Delta(1)\varpi(R)}{\Delta(1)} \tag{14}$$

  and the index of regularity, ρ, representing the entropy rate was computed as:

$$\rho = 1 - \min(\widetilde{\Delta}(R)) \tag{15}$$

  where $\varpi(R)$ represents the approximated percentage of the coded integers in Υ_R occurring once and ρ ranges from 0 (maximum randomness) to 1 (maximum regularity).

- The cross-entropy rate, ($\Lambda_{X|Y}$), estimates the entropy rate between two stochastic processes [40], [41]. In other words, it informs us about how accurately we can predict a data point in one signal based on a sequence of current and past data points in the other signal. The same normalization, quantization and coding steps performed for the entropy rate are repeated for two signals, X and Y. Then, we calculated

Shannon entropies of Υ_L^R, Υ_R^Y, and $\Upsilon_R^{X|Y}$, given by $\Delta_X(R)$, $\Delta_Y(R)$, and $\Delta_{X/Y}(R)$, respectively. These values of Shannon entropies were used to compute the normalized cross-entropy as follows:

$$\widetilde{\Delta}_{X|Y}(R) = \frac{\Delta_{X|Y}(R) - \Delta_Y(R-1) + \Delta_X(1) perc_{X|Y}(R)}{\Delta_X(1)} \tag{16}$$

where $\varpi_{X|Y}(L)$ represents the approximated percentage of the elements occurring only once in $\Upsilon_R^{X|Y}$. The normalized cross-entropy was then employed to calculate the uncoupling function as follows:

$$UF_{X,Y}(R) = \min\left(\widetilde{\Delta}_{X|Y}(R), \widetilde{\Delta}_{Y|X}(R)\right) \tag{17}$$

and the index of synchronization denoting the cross-entropy rate was calculated as:

$$\Lambda_{X|Y} = 1 - \min\left(UF_{X,Y}(R)\right). \tag{18}$$

$\Lambda_{X|Y}$ values range from 0 (X and Y are completely uncoupled) to 1 (perfect synchronization).

2.3.3 Frequency features

Three features, previously considered in other contributions (e.g., [42]), were computed in the frequency domain:

- The peak frequency, denoting a frequency at which the maximum spectral power occurred, was evaluated using the following relationship:

$$f_p = \arg \max_{f \in [0, f_{max}]} |F_X(f)|^2 \tag{19}$$

where $F_X(f)$ is the Fourier transform of the signal X and $f_{max} = 100$ Hz.

- The spectral centroid was evaluated as:

$$\hat{f} = \frac{\int_0^{f_{max}} f|F_X(f)|^2 \, df}{\int_0^{f_{max}} |F_X(f)|^2 \, df} \tag{20}$$

- In the current study, we defined the bandwidth of the signal using the following definition:

$$BW = \sqrt{\frac{\int_0^{f_{max}} \left(f - \hat{f}\right)^2 |F_X(f)|^2 \, df}{\int_0^{f_{max}} |F_X(f)|^2 \, df}} \tag{21}$$

2.3.4 Time-frequency features

The current study employed typical time-frequency features considered elsewhere (e.g., [24], [43]):

- The wavelet transform was utilized to learn about relative energies in different time-frequency bands. We used a 10-level discrete wavelet decomposition of the signal via the discrete Meyer wavelet (e.g.,

[44], [45], [46]) to compute the relative energy in each time-frequency band. In particular, the energy described by the approximation coefficients was computed as follows:

$$E_{a_{10}} = ||a_{10}||^2 \tag{22}$$

where $||\bullet||$ is the Euclidean norm and a_{10} represents a vector containing wavelet approximation coefficients at the tenth level. The energy described by the k^{th}-level detail coefficients was calculated by:

$$E_{d_k} = ||d_k||^2 \tag{23}$$

Lastly, we utilized the following two relations to compute the relative energy contribution from each decomposition level:

$$\Phi_a = \frac{E_{a_{10}}}{E_{a_{10}} + \sum_{k=1}^{10} E_{d_k}} \times 100\% \tag{24}$$

$$\Phi_{d_k} = \frac{E_{d_k}}{E_{a_{10}} + \sum_{k=1}^{10} E_{d_k}} \times 100\% \tag{25}$$

- The wavelet entropy computed as follows [24], [47]:

$$\Theta_X = -\Phi_{a_{10}} \log_2 \Phi_{a_{10}} - \sum_{k=1}^{10} \Phi_{d_k} \log_2 \Phi_{d_k} \tag{26}$$

utilized the same 10-level discrete wavelet decomposition as for the wavelet energy features above and is generally considered to be a measure of the degree of time-frequency based order-disorder of the signal. For example, a periodic mono-frequency signal can be considered as a very ordered process and its wavelet representation is usually provided by one unique wavelet resolution level. For such a signal, Θ_X will be of a very low value (near zero). However, a random process represents a very disordered behavior its wavelet representation will have with significant equivalent contributions from all frequency bands. Therefore, Θ_X for such a signal will reach very high values.

A summary of all measures and their meanings can be found in Table 1.

2.4 Statistical tests

To test for walk differences in the extracted features between groups and across directions, we initially used the Kruskal-Wallis test (e.g., [48]). Subsequently, we employed the Mann-Whitney test for pairwise comparisons between groups (e.g., [49]). A p-value of 0.05 was used to test for statistical significance. Given the exploratory nature of the study, no adjustments to the significant level for multiple comparisons were made.

3 Results

The results of our analysis are presented below.

3.1 Features based on stride intervals

The gait speed (GS) was statistically lower for PDs than for PNs ($p = 0.03$) as shown in Table 2. Regardless of group, the mean stride intervals (MSI) extracted from toes or heels were statistically equivalent (KW test, $p > 0.99$). Additionally, the CVs of stride intervals were not statistically different between the intervals extracted based on toes or heels (KW test, $p > 0.30$). Therefore, for the rest of the analysis, the stride intervals from the right toe are used.

The largest Lyapunov exponents were not affected by the location of the marker on the foot ($p > 0.397$). Furthermore, there were no group differences ($p > 0.11$). Harmonic ratios (HR) exhibited group statistical differences in the AP direction. HR_{AP} was statistically different between HCs and PDs ($p << 0.01$).

3.2 Statistical features

Table 4 summarizes the results for the considered statistical features based on gait accelerometry signals. Sample gait signals are shown in Figure 3. When considering the variability of gait accelerometric signals, σ, we observed no group differences in any directions ($p > 0.11$). However, the variability of these signals was statistically different between the three anatomical directions for all three groups ($p < 0.05$), with the accelerations in the V direction having the greatest variability ($p << 0.01$). When measuring the asymmetry of gait accelerometry data, we observed that there were group differences for ξ_{ML} between HCs and PDs ($p = 0.03$). The strongest asymmetry was in the V direction for all three groups ($p << 0.01$), but ξ_{ML} and ξ_{AP} were not statistically different for PDs. The behavior of the extreme points in the distributions depicting gait accelerometry data was measured with kurtossis, which showed that there were γ_{AP} group differences between HCs and PDs ($p < 0.02$). Furthermore, only HCs had statistically different kurtosis between the V and ML directions and the V and AP directions ($p < 0.01$). Other groups had no statistical differences between the directions. Lastly, when considering correlations between the three directions, there were no statistical differences between the groups ($p > 0.17$), but for PNs, η_{V-AP} was statistically higher than η_{ML-V} and η_{ML-AP} ($p < 0.01$).

3.3 Information-theoretic features

Information-theoretic features are shown in Table 5. Predictability of gait accelerometric signals (LZC) showed that accelerations signals in the ML direction were less complex for HCs than for PDs ($p = 0.01$) or for PNs ($p = 0.04$). Similarly, the acceleration signals in the AP direction had lower predictability than signals in the ML direction for all three groups ($p < 0.04$). Furthermore, the predictability was also smaller in the V direction than in the ML direction for HCs ($p << 0.01$), and but greater than the AP direction for PDs ($p = 0.02$).

Randomness of these accelorometric signals examined through the entropy rate of these signals found that there were group differences for ρ_{ML} between HCs and PN/PDs ($p < 0.04$). When considering the anatomical directions, HCs had more random acceleration in the ML direction than the V and AP directions

($p < 0.01$). For PNs, the ML direction only had statistical differences from the AP direction ($p = 0.04$). PDs had no statistical differences in different directions ($p > 0.06$).

To examine coupling between the three anatomical directions, we examined the cross-entropy rates which showed no significant differences between directions ($p > 0.17$) and between the groups ($p > 0.08$).

3.4 Frequency features

The frequency characteristics, summarized in Table 6, depict the frequency content of gait accelerometry signals for the groups. The peak frequencies were not statistically different among the groups in any direction ($p = 0.11$). The peak frequency in the ML direction is significantly lower than the peak frequency in the other two directions for all three groups ($p < 0.02$). There were no group differences in the spectral centroids in the ML and V directions ($p = 0.11$), but HCs had statistically lower spectral centroids in the AP direction than the PNs and PDs ($p < 0.04$). Furthermore, $\hat{f}_V$ was statistically lower than $\hat{f}_{ML}$ for all three groups ($p \leq 0.04$), and was statistically lower than $\hat{f}_{AP}$ for PNs and PDs ($p \leq 0.01$). Bandwidth differed among the three groups, depending upon the direction. Specifically, HCs had smaller bandwidths in the ML and AP directions than PNs/PDs ($p \leq 0.04$). The bandwidth in the V direction was statistically smaller than for the AP and ML directions for PNs and PDs ($p \leq 0.02$) and it was statistically smaller than the bandwidth in the AP direction for HCs ($p = 0.04$).

3.5 Time-frequency features

When considering the energy distribution across different wavelet bands (i.e., different time-frequency bands), PNs and PDs had statistically lower energy concentration in Φ_{MLd_7} of the ML direction than HCs ($p \leq 0.02$). The signals from the V direction had a different time-frequency structure since most of the energy (more than 99%) was concentrated in the approximation coefficients. Hence, we omitted the other coefficients from the analysis, since they did not provide any significant energy. No statistically different results were achieved in the AP direction.

There were no group differences in the wavelet entropies in all three directions ($p > 0.15$). It is also interesting to note that the signals in the V direction have their wavelet entropies close to zero, while in the ML directions the wavelet entropies are significantly higher ($p << 0.01$). Furthermore, PDs and HCs had statistically smaller entropies in the AP direction than in comparison to the ML direction ($p \leq 0.04$).

3.6 A summary table

Table 8 summarizes all our findings. Most of the proposed features were able to differentiate between healthy controls and PDs/PNs. The features were also able to differentiate among the three directions in some cases. However, none of the features was able to distinguish between PNs and PDs.

4 Discussion

We successfully acquired and extracted multiple features from trunk acceleration data in healthy adults and individuals with PD and PN during preferred pace treadmill walking. This is the first study to extract and report these features simultaneously, and to provide initial comparison of features between healthy and clinical groups and between directions of motion.

As expected, persons with PD walked more slowly than the other two groups; however, the other typical space-time stride interval features such as mean stride interval and coefficient of variation of stride interval failed to distinguish between the groups. In contrast, the features of the acceleration signal performed better, consistent with previous findings that acceleration measures (e.g., [7]) are often a more sensitive indicator of age- and disease-related changes in gait.

Several of the acceleration features, including harmonic ratios, skewness, kurtosis, LZC, entropy, the centroid frequency, bandwidth, and wavelet bands, were able to distinguish between the healthy controls and the clinical groups. These measures appear to provide unique but complementary information. For example, consistent with previous research we found that healthy controls had higher harmonic ratios, i.e. greater step-to-step symmetry in the AP direction (and also in ML and V directions, but not significant) than individuals with PD [7]. At the same time, healthy controls exhibited greater complexity and randomness of ML accelerations than individuals with PD or individuals with PN. Greater complexity and randomness of ML accelerations is expected in healthy gait, as control of ML motion is thought to be under continuous feedback control allowing online step-to-step adjustments for effective balance control [50]. As AP and ML motion are biomechanically coupled, greater ML complexity/randomness (better online adjustments) and greater smoothness in forward progression was expected. For PD/PN, less ML complexity/randomness and loss of smoothness in forward progression was found.

In addition to looking at differences in acceleration features across groups it is also useful to examine directional responses within a group. For example, when examining entropy rate for healthy controls ML randomness was greater than AP and V randomness. For individuals with PN, ML randomness was greater than AP; however, there were no directional differences for PD. The higher values overall and the lack of directional differences in entropy in the PD group suggests that individuals with PD are limiting their degrees of freedom and are moving en bloc. Together, our findings suggest that acceleration data may be most useful when features are not interpreted in isolation but interpreted together, providing a more complete picture into the motor control of walking.

The frequency and time-frequency measures were different across the three anatomical directions. These differences stemmed from the physiological directions of accelerations (i.e., it is expected to have significantly different acceleration profiles in the anterior-posterior direction in comparison to the vertical direction). However, some of these features were also able to differentiate between the HCs and PNs/PDs.

Though we were able to distinguish between HC and the clinical groups, no measure was able to discriminate the gait patterns of individuals with PD and PN. One possible explanation is that examining gait

on a treadmill, which has been shown to regulate gait (i.e. decrease spatiotemporal variability) may have ameliorated the impact of PD on gait. While it has been suggested that trunk dynamics alone may serve as global indicators of overall gait quality, it is possible that findings from additional accelerometers at the head or arms would have revealed further insights into inter-segmental coordination and better discrimination between clinical groups. Future efforts should continue to examine these trunk acceleration features simultaneously and in larger samples to confirm our findings, to explore gait adaptability via extraction of these features during challenging gait conditions, and explore coordination during usual and challenging walking conditions via extraction of features from additional accelerometers. In addition, care should be taken when interpreting our results in general due to the small sample size and potential for type II error.

While this paper highlights the range of measures that can be extracted from trunk acceleration data, ultimately we hope to use this type of information to guide, individualize, and evaluate therapeutic exercise interventions for older adults and clinical populations with gait and balance disorders. For example, it may be important to explore if and how gait rehabilitation interventions change acceleration features such as harmonic ratios, complexity and randomness. While research has shown that traditional exercise interventions (flexibility, strength and aerobic training) improve gait speed in older adults [51], [52], [53], it may be that interventions that include a timing and coordination component that focus on improving motor control processes essential for stepping [54] improve both spatiotemporal and trunk acceleration features, and this may ultimately have a greater impact on improving overall function and disability.

5 Conclusions

In this article, we examined the suitability of multiple signal feature for the analysis of gait accelerometry signals. Particularly, we examined statistical, information-theoretic, frequency and time-frequency features. The results of our numerical analysis showed that these features provided a valuable insight into the understanding of gait patterns in healthy and pathological populations.

Acknowledgment

The work was supported by the Pittsburgh Older Americans Independence Center (NIA P30 AG024827).

References

[1] J. M. Guralnik, L. Ferrucci, C. F. Pieper, S. G. Leveille, K. S. Markides, G. V. Ostir, S. Studenski, L. F. Berkman, and R. B. Wallace, "Lower extremity function and subsequent disability," *The Journals of Gerontology Series A: Biological Sciences and Medical Sciences*, vol. 55, no. 4, pp. M221–M231, Apr. 2000.

[2] M. Cesari, S. B. Kritchevsky, B. W. H. J. Penninx, B. J. Nicklas, E. M. Simonsick, A. B. Newman, F. A. Tylavsky, J. S. Brach, S. Satterfield, D. C. Bauer, M. Visser, S. M. Rubin, T. B. Harris, and M. Pahor, "Prognostic value of usual gait speed in well-functioning older peopleresults from the health, aging and body composition study," *Journal of the American Geriatrics Society*, vol. 53, no. 10, pp. 1675–1680, Oct. 2005.

[3] S. Studenski, S. Perera, K. Patel, C. Rosano, K. Faulkner, M. Inzitari, J. Brach, J. Chandler, P. Cawthon, E. B. Connor, M. Nevitt, M. Visser, S. Kritchevsky, S. Badinelli, T. Harris, A. B. Newman, J. Cauley, L. Ferrucci, and J. Guralnik, "Gait speed and survival in older adults," *JAMA: The Journal of the American Medical Association*, vol. 305, no. 1, pp. 50–58, Jan. 2011.

[4] T. Buracchio, H. H. Dodge, D. Howieson, D. Wasserman, and J. Kaye, "The trajectory of gait speed preceding mild cognitive impairment," *Archives of Neurology*, vol. 67, no. 8, pp. 980–986, Aug. 2010.

[5] B. R. Bloem, Y. A. M. Grimbergen, M. Cramer, M. Willemsen, and A. H. Zwinderman, "Prospective assessment of falls in Parkinson's disease," *Journal of Neurology*, vol. 248, no. 11, pp. 950–958, Nov. 2001.

[6] J. K. Richardson and E. A. Hurvitz, "Peripheral neuropathy: a true risk factor for falls," *The Journals of Gerontology Series A: Biological Sciences and Medical Sciences*, vol. 50, no. 4, pp. M211–M215, Jul. 1995.

[7] K. A. Lowry, A. L. Smiley-Oyen, A. J. Carrel, and J. P. Kerr, "Walking stability using harmonic ratios in Parkinson's disease," *Movement Disorders*, vol. 24, no. 2, pp. 261–267, Jan. 2009.

[8] R. E. Van Emmerik, R. C. Wagenaar, A. Winogrodzka, and E. C. Wolters, "Identification of axial rigidity during locomotion in parkinson disease," *Archives of Physical Medicine and Rehabilitation*, vol. 80, no. 2, pp. 186–191, Feb. 1999.

[9] T. K. DeMott, J. K. Richardson, S. B. Thies, and J. A. Ashton-Miller, "Falls and gait characteristics among older persons with peripheral neuropathy," *American Journal of Physical Medicine and Rehabilitation*, vol. 86, no. 2, pp. 125–132, Feb. 2007.

[10] M. D. Latt, H. B. Menz, V. S. Fung, and S. R. Lord, "Acceleration patterns of the head and pelvis during gait in older people with Parkinson's disease: A comparison of fallers and nonfallers," *The Journals of Gerontology: Series A*, vol. 64A, no. 6, pp. 700–706, Jun. 2009.

[11] M. E. Morris, J. McGinley, F. Huxham, J. Collier, and R. Iansek, "Constraints on the kinetic, kinematic and spatiotemporal parameters of gait in parkinson's disease," *Human Movement Science*, vol. 18, no. 23, pp. 461–483, Jun. 1999.

[12] I. P. I. Pappas, T. Keller, S. Mangold, M. R. Popovic, V. Dietz, and M. Morari, "A reliable gyroscope-based gait-phase detection sensor embedded in a shoe insole," *IEEE Sensors Journal*, vol. 4, no. 2, pp. 268–274, Apr. 2004.

[13] E. B. Titianova, P. S. Mateev, and I. M. Tarkka, "Footprint analysis of gait using a pressure sensor system," *Journal of Electromyography and Kinesiology*, vol. 14, no. 2, pp. 275 – 281, Apr. 2004.

[14] M. Henriksen, H. Lund, R. Moe-Nilssen, H. Bliddal, and B. Danneskiod-Samsoe, "Test-retest reliability of trunk accelerometric gait analysis," *Gait and Posture*, vol. 19, no. 3, pp. 288–297, Jun. 2004.

[15] R. Moe-Nilssen and J. L. Helbostad, "Estimation of gait cycle characteristics by trunk accelerometry," *Journal of Biomechanics*, vol. 37, no. 1, pp. 121–126, Jan. 2004.

[16] A. Hartmann, K. Murer, R. A. de Bie, and E. D. de Bruin, "Reproducibility of spatio-temporal gait parameters under different conditions in older adults using a trunk tri-axial accelerometer system," *Gait and Posture*, vol. 30, no. 3, pp. 351–355, Oct. 2009.

[17] A. E. Patla, A. Adkin, and T. Ballard, "Online steering: coordination and control of body center of mass, head and body reorientation," *Experimental Brain Research*, vol. 129, no. 129, pp. 629–634, Dec. 1999.

[18] D. A. Winter, C. D. MacKinnon, G. K. Ruder, and C. Wieman, "An integrated EMG/biomechanical model of upper body balance and posture during human gait," *Progress in Brain Research*, vol. 97, pp. 359–367, 1993.

[19] H. G. Kang and J. B. Dingwell, "Dynamic stability of superior vs. inferior segments during walking in young and older adults," *Gait and Posture*, vol. 30, no. 2, pp. 260–263, Aug. 2009.

[20] C. Hodt-Billington, J. L. Helbostad, and R. Moe-Nilssen, "Should trunk movement or footfall parameters quantify gait asymmetry in chronic stroke patients?" *Gait and Posture*, vol. 27, no. 4, pp. 552–558, May 2008.

[21] R. Moe-Nilssen and J. L. Helbostad, "Interstride trunk acceleration variability but not step width variability can differentiate between fit and frail older adults," *Gait and Posture*, vol. 21, no. 2, pp. 164–170, 2005.

[22] J. S. Brach, D. McGurl, D. Wert, J. M. VanSwearingen, S. Perera, R. Cham, and S. Studenski, "Validation of a measure of smoothness of walking," *The Journals of Gerontology Series A: Biological Sciences and Medical Sciences*, vol. 66A, no. 1, pp. 136–141, Jan. 2011.

[23] E. Sejdić, C. M. Steele, and T. Chau, "A method for removal of low frequency components associated with head movements from dual-axis swallowing accelerometry signals," *PLoS ONE*, vol. 7, no. 3, pp. e33 464–1–8, Mar. 2012.

[24] J. Lee, E. Sejdić, C. Steele, and T. Chau, "Effects of liquid stimuli on dual-axis swallowing accelerometry signals in a healthy population," *BioMedical Engineering OnLine*, vol. 9, no. 1, pp. 7–1–14, Feb. 2010.

[25] M. N. Nyan, F. E. H. Tay, K. H. W. Seah, and Y. Y. Sitoh, "Classification of gait patterns in the time-frequency domain," *Journal of Biomechanics*, vol. 39, no. 14, pp. 2647–2656, 2006.

[26] D. J. Thurman, P. A. S. Judd, and J. K. Rao, "Practice parameter: Assessing patients in a neurology practice for risk of falls (an evidence-based review) report of the quality standards subcommittee of the American Academy of Neurology," *Neurology*, vol. 70, no. 6, pp. 473–479, Feb. 2008.

[27] N. Fusco and A. Cretual, "Instantaneous treadmill speed determination using subjects kinematic data," *Gait and Posture*, vol. 28, no. 4, pp. 663–667, Nov. 2008.

[28] M. D. Chang, E. Sejdić, V. Wright, and T. Chau, "Measures of dynamic stability: Detecting differences between walking overground and on a compliant surface," *Human Movement Science*, vol. 29, no. 6, pp. 977–986, Dec. 2010.

[29] J. A. Fairley, E. Sejdić, and T. Chau, "The effect of treadmill walking on the stride interval dynamics of children," *Human Movement Science*, vol. 29, no. 6, pp. 987–998, Dec. 2010.

[30] M. T. Rosenstein, J. J. Collins, and C. J. De Luca, "A practical method for calculating largest Lyapunov exponents from small data sets," *Physica D: Nonlinear Phenomena*, vol. 65, no. 12, pp. 117–134, May 1993.

[31] M. B. Kennel, R. Brown, and H. D. I. Abarbanel, "Determining embedding dimension for phase-space reconstruction using a geometrical construction," *Physical Review A*, vol. 45, no. 6, pp. 3403–3411, Mar. 1992.

[32] J. B. Dingwell, J. P. Cusumano, P. R. Cavanagh, and D. Sternad, "Local dynamic stability versus kinematic variability of continuous overground and treadmill walking," *Journal of Biomechanical Engineering*, vol. 123, pp. 27–32, Feb. 2001.

[33] H. B. Menz, S. R. Lord, and R. C. Fitzpatrick, "Acceleration patterns of the head and pelvis when walking on level and irregular surfaces," *Gait and Posture*, vol. 18, no. 1, pp. 35–46, Aug. 2003.

[34] A. Papoulis, *Probability, Random Variables, and Stochastic Processes*, 3rd ed. New York: WCB/McGraw-Hill, 1991.

[35] M. Aboy, R. Hornero, D. Abasolo, and D. Alvarez, "Interpretation of the Lempel-Ziv complexity measure in the context of biomedical signal analysis," *IEEE Transactions on Biomedical Engineering*, vol. 53, no. 11, pp. 2282–2288, Nov. 2006.

[36] A. Porta, G. Baselli, D. Liberati, N. Montano, C. Cogliati, T. Gnecchi-Ruscone, A. Malliani, and S. Cerutti, "Measuring regularity by means of a corrected conditional entropy in sympathetic outflow," *Biological Cybernetics*, vol. 78, no. 1, pp. 71–78, Jan. 1998.

[37] A. Lempel and J. Ziv, "On the complexity of finite sequences," *IEEE Transactions on Information Theory*, vol. 22, no. 1, pp. 75–81, Jan. 1976.

[38] R. Ferenets, T. Lipping, A. Anier, V. Jantti, S. Melto, and S. Hovilehto, "Comparison of entropy and complexity measures for the assessment of depth of sedation," *IEEE Transaction on Biomedical Engineering*, vol. 53, no. 6, pp. 1067–1077, Jun. 2006.

[39] A. Porta, S. Guzzetti, N. Montano, R. Furlan, M. Pagani, A. Malliani, and S. Cerutti, "Entropy, entropy rate, and pattern classification as tools to typify complexity in short heart period variability series," *IEEE Transactions on Biomedical Engineering*, vol. 48, no. 11, pp. 1282–1291, Nov. 2001.

[40] A. Porta, S. Guzzetti, N. Montano, M. Pagani, V. Somers, A. Malliani, G. Baselli, and S. Cerutti, "Information domain analysis of cardiovascular variability signals: Evaluation of regularity, synchronisation and co-ordination," *Medical and Biological Engineering and Computing*, vol. 38, no. 2, pp. 180–188, Mar. 2000.

[41] A. Porta, G. Baselli, F. Lombardi, N. Montano, A. Malliani, and S. Cerutti, "Conditional entropy approach for the evaluation of the coupling strength," *Biological Cybernetics*, vol. 81, no. 2, pp. 119–129, Aug. 1999.

[42] E. Sejdić, C. M. Steele, and T. Chau, "The effects of head movement on dual-axis cervical accelerometry signals," *BMC Research Notes*, vol. 3, pp. 269–1–6, 2010.

[43] E. Sejdić, I. Djurović, and J. Jiang, "Time-frequency feature representation using energy concentration: An overview of recent advances," *Digital Signal Processing*, vol. 19, no. 1, pp. 153–183, Jan. 2009.

[44] M. Vetterli and J. Kovačević, *Wavelets and Subband Coding*. Englewood Cliffs, NJ: Prentice Hall, 1995.

[45] S. Stanković, I. Orović, and E. Sejdić, *Multimedia Signals and Systems*. New York, NY: Springer US, 2012.

[46] A. Cohen and J. Kovačević, "Wavelets: The mathematical background," *Proceedings of the IEEE*, vol. 84, no. 4, pp. 514–522, Apr. 1996.

[47] O. A. Rosso, S. Blanco, J. Yordanova, V. Kolev, A. Figliola, M. Schurmann, and E. Basar, "Wavelet entropy: a new tool for analysis of short duration brain electrical signals," *Journal of Neuroscience Methods*, vol. 105, no. 1, pp. 65–75, Jan. 2001.

[48] W. H. Kruskal and W. A. Wallis, "Use of ranks in one-criterion analysis of variance," *Journal of the American Statistical Association*, vol. 47, no. 260, pp. 583–621, Dec. 1952.

[49] H. B. Mann and D. R. Whitney, "On a test of whether one of two random variables is stochastically larger than the other," *The Annals of Mathematical Statistics*, vol. 18, no. 1, pp. 50–60, Mar. 1947.

[50] C. E. Bauby and A. D. Kuo, "Active control of lateral balance in human walking," *Journal of Biomechanics*, vol. 33, no. 11, pp. 1433–1440, Nov. 2000.

[51] C.-H. Chou, C.-L. Hwang, and Y.-T. Wu, "Effect of exercise on physical function, daily living activities, and quality of life in the frail older adults: A meta-analysis," *Archives of Physical Medicine and Rehabilitation*, vol. 93, no. 2, pp. 237–244, 2012.

[52] J. L. Helbostad, O. Sletvold, and R. Moe-Nilssen, "Home training with and without additional group training in physically frail old people living at home: effect on health-related quality of life and ambulation," *Clinical Rehabilitation*, vol. 18, no. 5, pp. 498–508, May 2004.

[53] T. Valenzuela, "Efficacy of progressive resistance training interventions in older adults in nursing homes: A systematic review," *Journal of the American Medical Directors Association*, vol. 13, no. 5, pp. 418–428, Jun. 2012.

[54] J. M. VanSwearingen, S. Perera, J. S. Brach, R. Cham, C. Rosano, and S. A. Studenski, "A randomized trial of two forms of therapeutic activity to improve walking: Effect on the energy cost of walking," *The Journals of Gerontology Series A: Biological Sciences and Medical Sciences*, vol. 64A, no. 11, pp. 1190–1198, Nov. 2009.

Figure captions

Figure 1 - Marker locations.

Figure 2 - Placement of the accelerometer over the L3 segment. Please note that subscript ML (mediolateral) denotes the x-axis of an accelerometer (positive to the right); the subscript V (vertical) denotes the y-axis of an accelerometer (positive upwards); and the subscript AP (anterior-posterior) denotes the z-axis of an accelerometer (positive posteriorly).

Figure 3 - Sample gait accelerometry signals: (a), (d) and (g) represent sample signals from HC in the A-P, V and M-L directions, respectively. (b), (e) and (h) represent sample signals from PN in the A-P, V and M-L directions, respectively. (c), (f) and (i) represent sample signals from PD in the A-P, V and M-L directions, respectively. The amplitude is expressed in **g**.

Figure 1

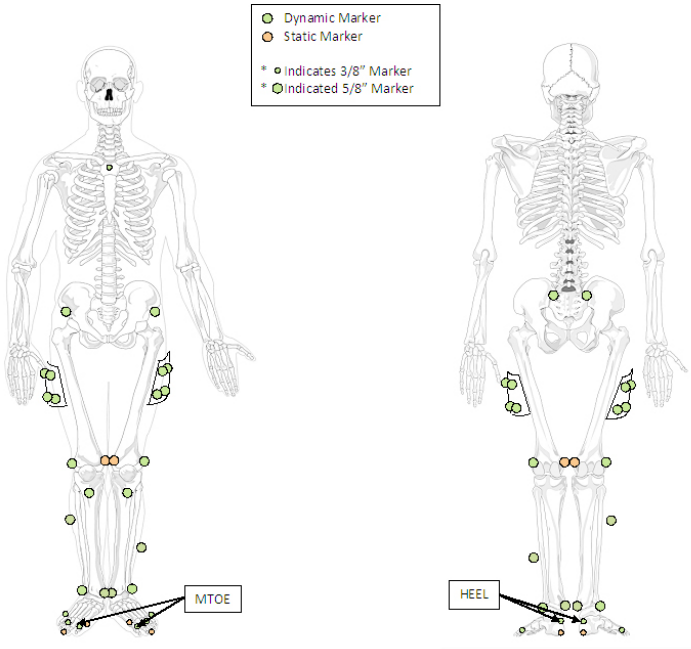

Figure 1: Marker locations.

Figure 2

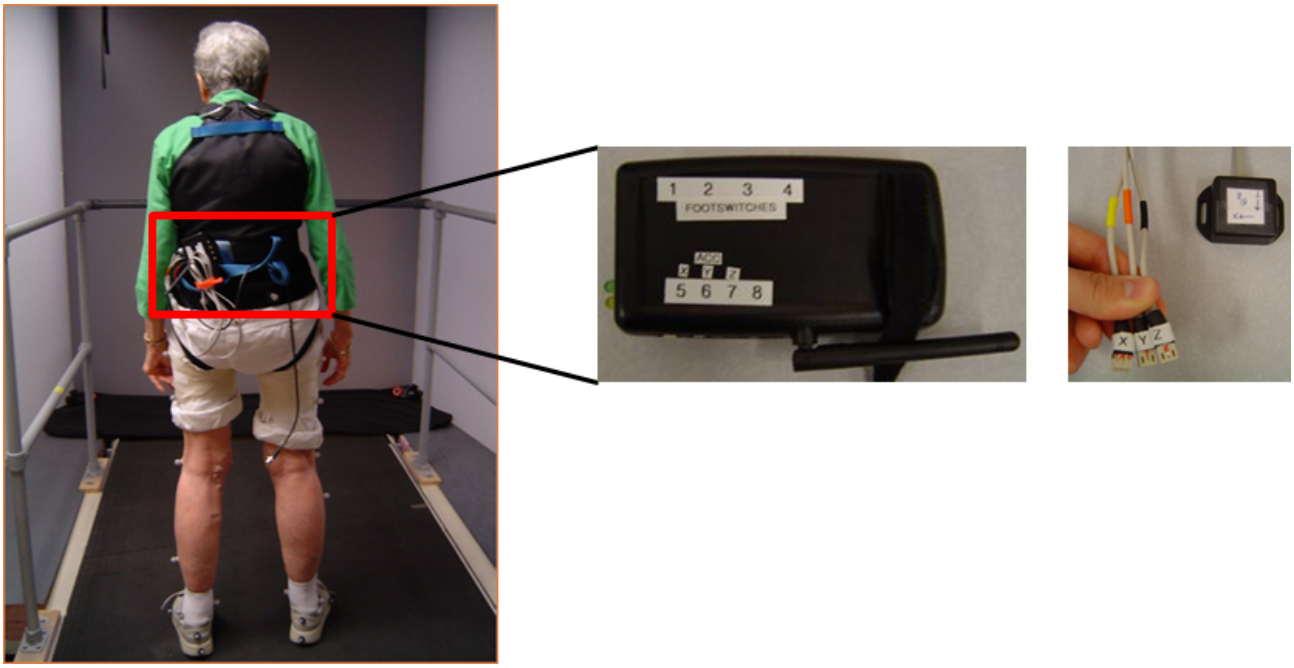

Figure 2: Placement of the accelerometer over the L3 segment. Please note that subscript ML (mediolateral) denotes the x-axis of an accelerometer (positive to the right); the subscript V (vertical) denotes the y-axis of an accelerometer (positive upwards); and the subscript AP (anterior-posterior) denotes the z-axis of an accelerometer (positive posteriorly).

Figure 3

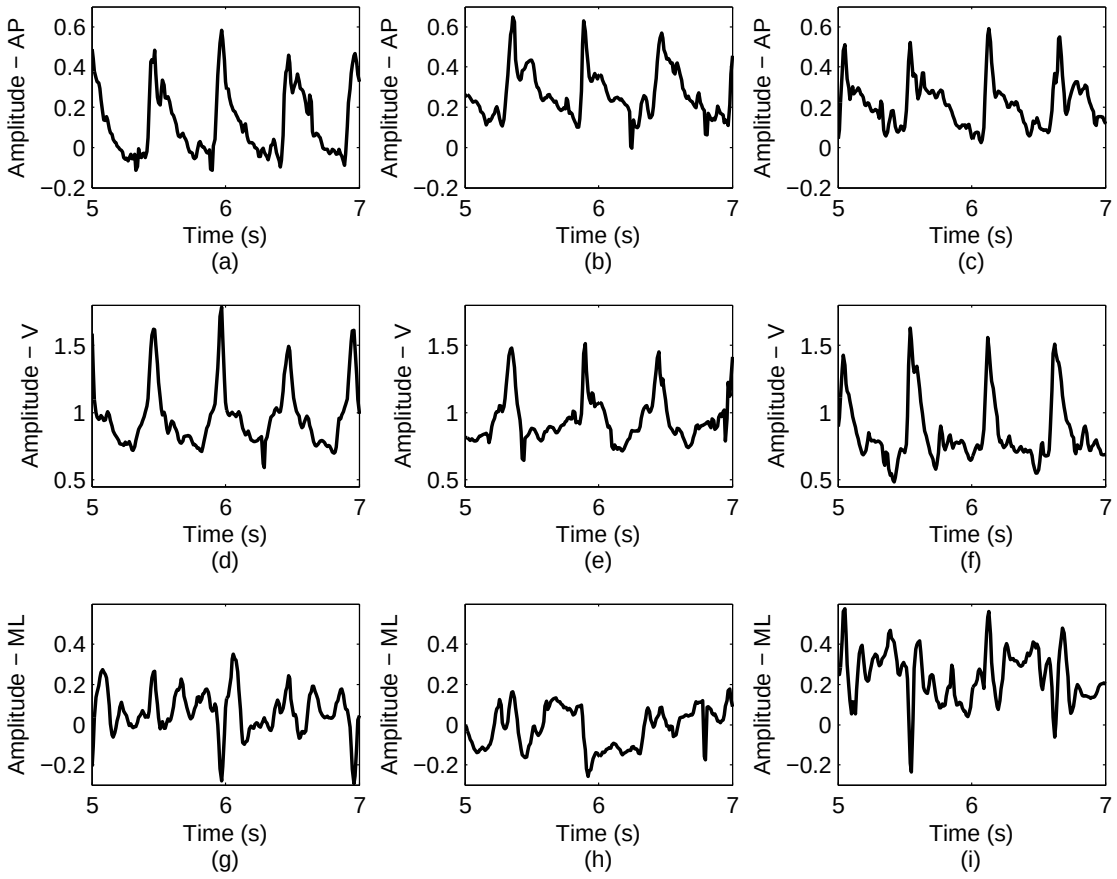

Figure 3: Sample gait accelerometry signals: (a), (d) and (g) represent sample signals from HC in the A-P, V and M-L directions, respectively. (b), (e) and (h) represent sample signals from PN in the A-P, V and M-L directions, respectively. (c), (f) and (i) represent sample signals from PD in the A-P, V and M-L directions, respectively. The amplitude is expressed in **g**.

Table captions

Table 1 - A summary of all features implemented in the study.

Table 2 - Values of basic SI features. GS = gait speed; MSI = mean stride interval; CV = coefficient of variation for stride intervals. † = statistical differences between PNs and PDs.

Table 3 - Variations of the largest Lyapunov exponents and harmonic ratios among different groups. ‡ = statistical differences between HCs and PDs.

Table 4 - Values of basic statistical features for accelerometry signals. ‡ = statistical differences between HCs and PDs.

Table 5 - Variations of information-theoretic features during various walking tasks. ‡ = statistical differences between HCs and PDs. § = statistical differences between HCs and PDs.

Table 6 - Frequency variations during various walking tasks. ‡ = statistical differences between HCs and PDs. § = statistical differences between HCs and PDs.

Table 7 - Time-frequency variations of gait accelerometry signals during various walking tasks. ‡ = statistical differences between HCs and PDs. § = statistical differences between HCs and PDs.

Table 8 - A summary of all features implemented in the study.

Table 1

Table 1: A summary of all features implemented in the study.

Feature and abbreviation	**Definition**
Gait speed (GS)	Distance walked per unit of time (m/s).
Mean stride interval (MSI)	Duration of a stride averaged over all strides.
Coefficient of variation of the stride interval (CV)	(Within-subject standard deviation of the stride interval divided by the mean stride interval)$\times$100%
Lyapunov exponents ($\lambda_{L_{ML}}$, $\lambda_{L_{AP}}$, λ_{L_V})	Quantifies local dynamic stability; the average exponential rate of divergence based on naturally occurring local perturbations.
Harmonic ratios (HR_{ML}, HR_{AP}, HR_V)	Quantifies the harmonic composition of the accelerations for a given stride via DFT; HRs are calculated using the first 20 harmonic coefficients; higher values are interpreted as greater walking smoothness.
Standard deviation of signal amplitude (σ_{ML}, σ_{AP}, σ_V)	Describes the spread of the amplitude distribution; higher values indicate a greater spread of amplitude values.
Skewness of signal amplitude (ξ_{ML}, ξ_{AP}, ξ_V)	Describes the asymmetry of amplitude distribution; negative skewness indicates that distribution of signal amplitudes lies predominantly on the right of the mean amplitude, positive skewness indicates the values are predominantly on the left of the mean amplitude.
Kurtosis of signal amplitude (γ_{ML}, γ_{AP}, γ_V)	Describes the extent to which the distribution of amplitudes is concentrated about the mean amplitude; higher kurtosis values indicate the distribution is more peaked, with infrequent extreme deviations.
Cross-correlation (η_{ML-V}, η_{ML-AP}, η_{AP-V})	Measures the agreement or similarity between 2 directional acceleration signals (e.g. AP and V accelerations); values range from 0-1 where 0 indicates no similarity and 1 indicates identical signals.
Lempel-Ziv complexity (LZC_{ML}, LZC_{AP}, LZC_V)	Measures the complexity-predictability of the signal; higher values indicate a less predictable, more complex signal, lower values indicate a more predictable less complex signal.
Entropy rate (ρ_{ML}, ρ_{AP}, ρ_V)	Quantifies the regularity of a signal when anticipated that consecutive data points are related; values range from 0-1 where 0 =maximum randomness/no relationship among consecutive data points, to 1 = maximum regularity.
Cross-entropy rate/index of synchronization ($\Lambda_{ML\|V}$, $\Lambda_{ML\|AP}$, $\Lambda_{AP\|V}$)	Quantifies the entropy rate between 2 acceleration signals/how accurately can we predict a data point in one signal given current and past data in the other signal; the index of synchronization ranges from 0-1 where 0 indicates the 2 signals are completely unsynchronized, and 1 reflects perfect synchronization.
Peak frequency (f_{pML}, f_{pAP}, f_{pV})	The maximum spectral power.
Centroid frequency ($\hat{f}_{ML}$, $\hat{f}_{AP}$, $\hat{f}_{ML}$)	The frequency that divides the spectral power distribution into two equal parts.
Bandwidth (BW_{ML}, BW_{AP}, BW_V)	The difference between the uppermost and lower most frequencies/range of frequencies in the signal.
Wavelet bands (Φ)	Measures the relative energy contribution in a time-frequency band.
Wavelet entropy (Θ_{ML}, Θ_{AP}, Θ_V)	Quantifies the degree signal disorder in the time-frequency domain; high values represent disordered behavior with significant equivalent contributions from all frequency bands (e.g. random process).

Table 2

Table 2: Values of basic SI features. GS = gait speed; MSI = mean stride interval; CV = coefficient of variation for stride intervals. † = statistical differences between PNs and PDs.

	HC	PN	PD
GS	1.09 ± 0.11	1.13 ± 0.08	$0.96 \pm 0.16^{\dagger}$
MSI	1.11 ± 0.10	1.10 ± 0.07	1.14 ± 0.08
CV	2.29 ± 0.57	2.29 ± 0.56	2.33 ± 0.96

Table 3

Table 3: Variations of the largest Lyapunov exponents and harmonic ratios among different groups. ‡ = statistical differences between HCs and PDs.

	HC	PN	PD
$\lambda_{L_{ML}}$	0.01 ± 0.01	0.02 ± 0.01	0.01 ± 0.01
λ_{L_V}	0.02 ± 0.05	0.01 ± 0.01	0.01 ± 0.01
$\lambda_{L_{AP}}$	0.01 ± 0.03	0.01 ± 0.02	0.02 ± 0.02
HR_{ML}	2.34 ± 0.56	1.90 ± 0.44	1.89 ± 0.45
HR_V	$3.40 \pm 0.96^{\ddagger}$	2.99 ± 0.38	2.66 ± 0.55
HR_{AP}	3.03 ± 0.80	2.51 ± 0.50	2.16 ± 0.48

Table 4

Table 4: Values of basic statistical features for accelerometry signals. ‡ = statistical differences between HCs and PDs.

	HC	PN	PD
σ_{ML}	0.11 ± 0.02	0.11 ± 0.02	0.10 ± 0.02
σ_{V}	0.19 ± 0.05	0.19 ± 0.03	0.17 ± 0.03
σ_{AP}	0.14 ± 0.03	0.14 ± 0.03	0.12 ± 0.02
ξ_{ML}	$-0.12 \pm 0.21^{\ddagger}$	0.01 ± 0.27	0.05 ± 0.19
ξ_{V}	1.31 ± 0.44	1.19 ± 0.49	1.09 ± 0.35
ξ_{AP}	0.37 ± 0.54	0.39 ± 0.29	0.20 ± 0.48
γ_{ML}	4.07 ± 2.42	4.43 ± 2.03	5.08 ± 1.76
γ_{V}	5.51 ± 2.27	4.86 ± 1.11	4.86 ± 1.21
γ_{AP}	$4.00 \pm 1.50^{\ddagger}$	6.31 ± 5.37	6.54 ± 3.70
η_{ML-V}	0.14 ± 0.24	0.07 ± 0.15	0.25 ± 0.30
η_{ML-AP}	0.13 ± 0.20	0.09 ± 0.13	0.14 ± 0.25
η_{V-AP}	0.52 ± 0.39	0.63 ± 0.36	0.51 ± 0.46

Table 5

Table 5: Variations of information-theoretic features during various walking tasks. ‡ = statistical differences between HCs and PDs. § = statistical differences between HCs and PDs.

	N	PN	PD
LZC_{ML}	$0.58 \pm 0.06^{\ddagger}$	0.53 ± 0.05	0.52 ± 0.03
LZC_{V}	0.53 ± 0.05	0.51 ± 0.04	0.51 ± 0.02
LZC_{AP}	0.53 ± 0.05	0.49 ± 0.05	0.48 ± 0.03
ρ_{ML}	$0.63 \pm 0.13^{\ddagger}$	$0.73 \pm 0.08^{\S}$	0.77 ± 0.07
ρ_{V}	0.76 ± 0.06	0.76 ± 0.06	0.77 ± 0.04
ρ_{AP}	0.75 ± 0.09	0.80 ± 0.06	0.80 ± 0.04
$\Lambda_{ML\|V}$	0.80 ± 0.16	0.89 ± 0.13	0.91 ± 0.14
$\Lambda_{ML\|AP}$	0.77 ± 0.12	0.84 ± 0.17	0.89 ± 0.09
$\Lambda_{AP\|V}$	0.84 ± 0.18	0.83 ± 0.15	0.84 ± 0.10

Table 6

Table 6: Frequency variations during various walking tasks. ‡ = statistical differences between HCs and PDs. § = statistical differences between HCs and PDs.

	N	PN	PD
f_{pML}	1.56 ± 1.36	1.06 ± 0.49	0.88 ± 0.06
f_{pV}	1.82 ± 0.16	1.82 ± 0.12	1.76 ± 0.12
f_{pAP}	1.81 ± 0.16	1.82 ± 0.12	1.76 ± 0.12
$\hat{f}_{ML}$	6.46 ± 2.03	6.41 ± 1.58	7.49 ± 1.66
$\hat{f}_{V}$	5.07 ± 1.46	5.12 ± 0.92	5.49 ± 1.08
$\hat{f}_{AP}$	$5.59 \pm 1.35^{\ddagger}$	$7.40 \pm 2.67^{\S}$	7.77 ± 2.09
BW_{ML}	$7.50 \pm 2.12^{\ddagger}$	$9.22 \pm 2.06^{\S}$	9.97 ± 1.38
BW_{V}	6.26 ± 2.32	6.99 ± 1.60	7.30 ± 0.91
BW_{AP}	$7.89 \pm 2.16^{\ddagger}$	$9.86 \pm 2.44^{\S}$	10.4 ± 1.68

Table 7

Table 7: Time-frequency variations of gait accelerometry signals during various walking tasks. ‡ = statistical differences between HCs and PDs. § = statistical differences between HCs and PDs.

	HC	PN	PD
Φ_{MLd_7}	$12.1 \pm 8.44^{\ddagger}$	$5.21 \pm 5.16^{\S}$	3.96 ± 2.71
$\Phi_{Va_{10}}$	99.3 ± 0.32	99.3 ± 0.16	99.4 ± 0.25
Θ_{ML}	1.71 ± 0.70	1.42 ± 0.64	1.52 ± 0.54
Θ_{V}	0.08 ± 0.03	0.08 ± 0.01	0.07 ± 0.02
Θ_{AP}	0.99 ± 0.82	1.00 ± 0.76	0.87 ± 0.99

Table 8

Table 8: A summary of all features implemented in the study.

Feature	**Discriminates between healthy and disease?**	**Directional differences (within group)**
GS	Yes, PDs slower than PNs.	NA
MSI	No	NA
CV	No	NA
$\lambda_{L_{ML}}$, $\lambda_{L_{AP}}$, λ_{L_V}	No	No
HR_{ML}, HR_{AP}, HR_V	Yes, HCs have greater AP smoothness than PDs.	Yes for all groups (though not significant). The highest smoothness values were in the V direction, the lowest smoothness values were in the ML direction.
σ_{ML}, σ_{AP}, σ_V	No	Yes, for all groups the V direction had the greatest standard deviation of signal amplitude.
ξ_{ML}, ξ_{AP}, ξ_V	Yes, differences in ML skewness between HCs (negative skewness) and PDs (positive skewness).	Yes, for all groups the V direction had the largest positive skewness.
γ_{ML}, γ_{AP}, γ_V	Yes, HCs had lower AP kurtosis than PDs.	Yes, for HCs the V direction had significantly higher kurtosis than AP or ML.
η_{ML-V}, η_{ML-AP}, η_{AP-V}	No	Yes, all groups had the highest cross-correlation between V-AP, significant only for PNs.
LZC_{ML}, LZC_{AP}, LZC_V	Yes, HCs had greater ML complexity than PDs /PNs.	Yes, the ML direction had the most complexity for all 3 groups.
ρ_{ML}, ρ_{AP}, ρ_V	Yes, HCs had greater ML randomness than PDs/ PNs.	Yes, for HCs ML randomness was greater than AP or V; for PNs ML randomness was greater than AP only; no directional differences for PDs.
$\Lambda_{ML\|V}$, $\Lambda_{ML\|AP}$, $\Lambda_{AP\|V}$	No	No
f_{pML}, f_{pAP}, f_{pV}	No	Yes, the peak frequency was lowest in the ML direction for all groups.
$\hat{f}_{ML}$, $\hat{f}_{AP}$, $\hat{f}_{ML}$	Yes, HCs had a lower AP centroid frequency than PDs/PNs.	Yes, for all groups the V centroid frequency was the lowest and different from the ML frequency; for PDs/PNs the V frequency was also lower than the AP frequency.
BW_{ML}, BW_{AP}, BW_V	Yes, HCs had smaller ML and AP bandwidths than PDs/PNS.	Yes, for all groups the V bandwidth was the smallest and different from ML bandwidth; for PDs/PNs the V bandwidth was also smaller than AP bandwidth.
Φ	Yes, HCs had higher energy concentration in certain ML bands.	Yes, different time-frequency structure in the V direction.
Θ_{ML}, Θ_{AP}, Θ_V	No	Yes, for all groups the ML wavelet entropies were the highest and different from the V direction; for HCs /PDs the ML entropies were also higher than in the AP direction.